Long time simulation of a beam in a periodic focusing channel via a two-scale PIC-method

Emmanuel Frénod, Francesco Salvarani, Eric Sonnendrücker

Long time simulation of a beam in a periodic focusing channel via a two-scale PIC-method

E. Frénod* F. Salvarani† E. Sonnendrücker‡

October 22, 2007

Abstract

We study the two-scale asymptotics for a charged beam under the action of a rapidly oscillating external electric field. After proving the convergence to the correct asymptotic state, we develop a numerical method for solving the limit model involving two time scales and validate its efficiency for the simulation of long time beam evolution.

Keywords: Vlasov-Poisson system, kinetic equations, homogenization, two-scale convergence, two-scale PIC method.

AMS subject classifications: 82D10 (35B27 76X05)

1 Introduction

Charged particle beams, as used in beam physics for many applications ranging from heavy ion fusion to cancer therapy, often need to be transported on very long distances in particle accelerators. Moreover, as particles of the same charge repulse each other, these beams need to be focused using external electric or magnetic fields (see, for example, the paper of Filbet and Sonnendrücker [12] for a mathematical description of particle beam modelling and numerical simulation). Beam focusing can be performed either in linear or circular accelerators using a periodic focusing lattice.

The aim of this paper is to study the evolution of a beam over a large number of periods. The motion of electrically charged particles is governed by several phenomena: *in primis*, it is necessary to take into account the interactions between the electric fields generated by the particles themselves and by the external focusing electromagnetic field. The kinetic approach is a successful method suitable to model a system composed by a great number of particles; in our case the modelling framework will be given by coupling a kinetic equation with the Maxwell equation. When it is possible to disregard the collisions between particles, the kinetic part of the modelling analysis is performed by means of the Vlasov collisionless equation [13]. In this paper we will consider only non-relativistic long and thin beams; therefore, instead of studying the phenomenon by means of the full Vlasov-Maxwell system, we will consider its paraxial approximation. This simplified model of the Vlasov-Maxwell equations is particularly adapted to the study of long and thin beams and describes the evolution of a charged particle beam in the plane transverse to its direction of propagation.

The key assumptions of the paraxial approximation are the following:

*LMAM et Lemel, Université de Bretagne sud, Campus de Tohannic, 56000 Vannes, France

†Dipartimento di Matematica, Università degli Studi di Pavia. Via Ferrata, 1 - 27100 Pavia, Italy

‡Institut de Recherche Mathématique Avancée UMR 7501, Université Louis Pasteur, Strasbourg 1 et CNRS, et Projet Calvi INRIA Nancy - Grand Est, 7 rue Ren Descartes - 67084 Strasbourg Cedex, France

1. we suppose that there is a predominant length scale, namely the longitudinal length of the beam, whereas the transverse thickness of the beam is negligible with respect to its longitudinal length;

2. we will assume that the beam has already reached its stationary state.

Such assumptions are often verified in applications: in a standard accelerator, the orders of magnitude of the different lengths taken into account verify the first assumption; moreover it is often interesting to study stable (in time) configurations of the beam, and therefore the second assumption applies. In the paraxial framework, the effects of the self consistent magnetic and electric fields can be both taken into account by solving a single Poisson equation. Hence the model becomes similar to the Vlasov-Poisson system in the transverse plane with respect to the accelerator axis. In the paraxial model, the z coordinate plays the role of time. We will switch here to more conventional notations and consider the time-dependent two-dimensional Vlasov-Poisson system. We assume moreover, in accordance with most experiments, that the average external field is large compared to the self-consistent field. More details about the derivation of this model can be found in [4] or [12], whereas a more complete description on accelerators' physics can be found in the book by Davidson and Qin [3].

In the framework we just precised, the Vlasov-Poisson system takes the form

$$\begin{cases} \dfrac{\partial f_\varepsilon}{\partial t} + \dfrac{1}{\varepsilon}\mathbf{v}\cdot\nabla_x f_\varepsilon + (\mathbf{E}_\varepsilon + \boldsymbol{\Xi}^\varepsilon)\cdot\nabla_v f_\varepsilon = 0, \\ \mathbf{E}_\varepsilon = -\nabla\Phi_\varepsilon, \\ \Delta\Phi_\varepsilon = -\rho_\varepsilon(t,\mathbf{x}), \qquad \rho_\varepsilon(t,\mathbf{x}) = \displaystyle\int_{\mathbb{R}^2_v} f_\varepsilon(t,\mathbf{x},\mathbf{v})\,d\mathbf{v}, \\ f_\varepsilon(t=0,\mathbf{x},\mathbf{v}) = f_0, \end{cases} \tag{1}$$

where $f_\varepsilon = f_\varepsilon(t,\mathbf{x},\mathbf{v})$ is the distribution function, $t \in [0,T)$ for some $T < \infty$, $\mathbf{x} = (x_1,x_2) \in \mathbb{R}^2_x$ is the position vector and $\mathbf{v} = (v_1,v_2) \in \mathbb{R}^2_v$ is the velocity vector. We will denote by $\Omega = \mathbb{R}^2_x \times \mathbb{R}^2_v$.

As said before, we are working in a stationary setting. In this context, the variable t does not represent, from a physical point of view, a time variable, but rather the longitudinal coordinate. We have nevertheless chosen to use the variable t because of the great similarity of the paraxial approximation with respect to a two-dimensional (in space) time-dependent Vlasov equation. The electric field $\boldsymbol{\Xi}^\varepsilon(t,\mathbf{x})$ is supposed to be external, and has the form

$$\boldsymbol{\Xi}^\varepsilon(t,\mathbf{x}) = -\frac{1}{\varepsilon}H_0\mathbf{x} + H_1\left(\omega_1\frac{t}{\varepsilon}\right)\mathbf{K}\mathbf{x},$$

where H_0 is a positive constant and H_1 is $2\pi-$periodic, with mean value 0. $\mathbf{K}$ is a 2×2 symmetrical isometric matrix. In the two most common physical situations, $\mathbf{K} = I$ or $\mathbf{K} = \begin{pmatrix} 1 & 0 \\ 0 & -1 \end{pmatrix}$. The parameter ε is a scaling parameter acting on the "time" scale (i.e. the longitudinal scale). Its physical meaning will be detailed in the next section.

The form of the external electric field will satisfy some relevant physical requirements. The field which models the periodic focusing lattice needs indeed to be linear in $\mathbf{x}$ to compensate for the self field which is also linear in $\mathbf{x}$ for a uniform beam but with the opposite sign. The variation of the field with respect to t is assumed to be a small amplitude field oscillating at the same period as the lattice.

Under additional physical hypotheses, a simplified version of (1) may be considered. These assumptions consist, in the case when $\mathbf{K} = I$, in considering that the beam is axisymmetric, *i.e.* invariant under rotation in $\mathbb{R}^2_x$. Then, by writing (1.a) in polar coordinates (r, θ), such that $r = |\mathbf{x}|$, $x_1 = r\cos(\theta)$ and $x_2 = r\sin(\theta)$ we get

$$\frac{\partial f_\varepsilon}{\partial t} + \frac{1}{\varepsilon} v_r \frac{\partial f_\varepsilon}{\partial r} + \left(\mathbf{E}_{r\varepsilon} + \mathbf{\Xi}_r{}^\varepsilon + \frac{(r v_\theta)^2}{r^3} \right) \frac{\partial f_\varepsilon}{\partial v_r} = 0, \tag{2}$$

where v_r is the projection of the velocity on radius $\mathbf{x}$. In other words, $v_r = \mathbf{v}\cdot\mathbf{x}/r$ and $v_\theta = \mathbf{v}\cdot\mathbf{x}^\perp/r$ where $\mathbf{x}^\perp = (-x_2, x_1)$. If finally, f_ε is assumed to be concentrated in angular momentum $r v_\theta = 0$ (this property is achieved if the initial condition f_0 is concentrated in angular momentum), system (1) yields

$$\begin{cases} \dfrac{\partial f_\varepsilon}{\partial t} + \dfrac{1}{\varepsilon} v_r \dfrac{\partial f_\varepsilon}{\partial r} + (\mathbf{E}_{r\varepsilon} + \mathbf{\Xi}_r{}^\varepsilon) \dfrac{\partial f_\varepsilon}{\partial v_r} = 0, \\ \dfrac{1}{r} \dfrac{\partial (r \mathbf{E}_{r\varepsilon})}{\partial r} = \rho_\varepsilon(t, r), \qquad \rho_\varepsilon(t, r) = \displaystyle\int_{\mathbb{R}} f_\varepsilon(t, r, v_r)\, dv_r, \\ f_\varepsilon(t = 0, r, v_r) = f_0, \end{cases} \tag{3}$$

where $f_\varepsilon = f_\varepsilon(t, r, v_r)$ for $t \in [0, T)$, $r \in \mathbb{R}^+$ and $v_r \in \mathbb{R}$. The external force $\mathbf{\Xi}_r{}^\varepsilon$ writes here

$$\mathbf{\Xi}_r{}^\varepsilon(t, r) = \big(-\frac{1}{\varepsilon} H_0 + H_1\left(\omega_1 \frac{t}{\varepsilon}\right) \big) r.$$

System (3) is naturally set for $r \in \mathbb{R}^+$. Nevertheless, we can consider that $r \in \mathbb{R}$ using the convention $f_\varepsilon(t, r, v_r) = f_\varepsilon(t, -r, -v_r)$ and $\mathbf{\Xi}_r{}^\varepsilon(t, r) = \mathbf{\Xi}_r{}^\varepsilon(t, -r)$. This is what we do in the following.

The main purpose of the paper is the study of systems (1) and (3) in the limit as $\varepsilon \to 0$. We have chosen to work in the framework of the so-called two-scale convergence, an homogenization technique introduced by N'guetseng [14] and subsequently developed by Allaire [2] and Frénod, Raviart and Sonnendrücker [9], which essentially says that $f_\varepsilon(t, \mathbf{x}, \mathbf{v})$ is close to $F(t, t/\varepsilon, \mathbf{x}, \mathbf{v})$ for a given profile F. This notion is stronger than the usual weak or weak* convergence and is very adapted to the study of asymptotic behaviour of transport equations with rapidly oscillating terms, as was shown in [5, 8, 9, 10, 11]. On the other hand, we develop a numerical method in order to compute an approximation of f_ε. This method consists, in the spirit suggested in Frénod, Raviart and Sonnendrücker [9] and Frénod [6] and explored in Ailliot, Frénod and Monbet [1] and in Frénod, Mouton and Sonnendrücker [7], in computing the profile F by discretizing the equation it satisfies. Then an approximation of f_ε is reconstructed using $f_\varepsilon(t, \mathbf{x}, \mathbf{v}) \sim F(t, t/\varepsilon, \mathbf{x}, \mathbf{v})$. For simplicity reasons, the considered method is implemented in the simplified case of system (3). Nevertheless, it is easy to see that it may be adapted in a straightforward way to system (1) and others situations where multiple time scales are involved.

The paper is organized as follows: in Section 2 we obtain the scaled Vlasov-Poisson system (1) from the standard Vlasov-Poisson system by means of a scaling procedure. Section 3 is then devoted to the derivation of some useful properties of the solution of (1), whereas Section 4 is dedicated to homogenization of systems (1) and (3) by means of the two-scale convergence. Finally, in Section 5 we will implement and test the previously described numerical method based on the homogenization analysis.

2 Scaling of the Vlasov equation: the paraxial approximation

We present in this paragraph the scaling procedure leading to Equation (1). We first note that, in the formulation of the problem, there are different scales: the length of the accelerator L, the transverse radius of the beam λ and the period of the oscillating external field l. In a standard accelerator, the orders of magnitude of such quantities are: $L \simeq 10^3$ m; $l \simeq 10^{-1}$ m and, finally, $\lambda \simeq 10^{-2}$ m. The standard three-dimensional Vlasov-Poisson system, in presence of an external electric field $\mathbf{\Xi}$, is given by

$$\begin{cases} \dfrac{\partial f}{\partial t} + \mathbf{v} \cdot \nabla_x f + \dfrac{q}{m} (\mathbf{E} + \mathbf{\Xi}) \cdot \nabla_v f = 0, \\ \\ \mathbf{E} = -\nabla \Phi, \\ \\ \Delta \Phi = -\dfrac{1}{\varepsilon_0} \rho(t, \mathbf{x}), \qquad \rho(\mathbf{x}, t) = q \displaystyle\int_{\mathbb{R}^3_v} f(t, \mathbf{x}, \mathbf{v})\, d\mathbf{v}, \\ \\ f(t = 0, \mathbf{x}, \mathbf{v}) = f_0, \end{cases} \tag{4}$$

where $f \equiv f(t, \mathbf{x}, \mathbf{v})$ is the distribution function, $t \in [0, T)$ for some $T < \infty$, $\mathbf{x} = (x_1, x_2, x_3) \in \mathbb{R}^3_x$ is the position vector and $\mathbf{v} = (v_1, v_2, v_3) \in \mathbb{R}^3_v$ is the velocity vector.

The external electric field $\mathbf{\Xi} = \mathbf{\Xi}(\mathbf{x})$ is supposed to be independent of time and periodic with respect to the variable x_3. Under the paraxial approximation, f is supposed to be stationary with respect to time and the velocity of the particles with respect to the longitudinal direction of the beam (which will be $\mathbf{e}_3$ throughout the whole paper) is constant, that is $v_3 = v_b$. These assumptions will enable us to eliminate the time derivative in the first equation of (4) and suppose that $f(t, \mathbf{x}, \mathbf{v}) = f(\mathbf{x}, v_1, v_2) \otimes \delta(v_b - v_3)$. In order to obtain the dimensionless version of the Vlasov-Poisson system (4), we define the new variables x_i', v_i' by:

$$x_i = \lambda\, x_i', \qquad v_i = v_b\, v_i', \qquad i = 1,\, 2$$

$$x_3 = L\, x_3', \qquad v_3 = v_b.$$

Moreover, the dimensionless density f', external electric field $\mathbf{\Xi}'$, self-consistent electric field $\mathbf{E}'$ and its potential Φ' are defined by

$$f = \bar{f} f', \qquad \mathbf{\Xi} = \bar{\Xi}\, \mathbf{\Xi}', \qquad \mathbf{E} = \bar{E}\, \mathbf{E}', \qquad \Phi = \bar{\Phi}\, \Phi'.$$

Under such a change of variables, we obtain that the Vlasov-Poisson system (4) can be written in the following form:

$$\begin{cases} \dfrac{\bar{f} v_b}{L} \dfrac{\partial f'}{\partial x_3'} + \dfrac{\bar{f} v_b}{\lambda} \displaystyle\sum_{i=1}^{2} v_i' \frac{\partial f'}{\partial x_i'} + \frac{q \bar{E} \bar{f}}{m v_b} \sum_{i=1}^{2} \left(E_i' + \frac{\bar{\Xi}}{\bar{E}} \Xi_i' \right) \frac{\partial f'}{\partial v_i'} = 0, \\ \\ \bar{E} E_i' = -\dfrac{\bar{\Phi}}{\lambda} \dfrac{\partial \Phi'}{\partial x_i'}, \qquad i = 1,\ 2; \qquad \bar{E} E_3' = -\dfrac{\bar{\Phi}}{L} \dfrac{\partial \Phi'}{\partial x_3'}, \\ \\ \dfrac{\bar{\Phi}}{\lambda^2} \displaystyle\sum_{i=1}^{2} \left(\frac{\partial^2 \Phi'}{\partial x_i'^2} \right) + \frac{\bar{\Phi}}{L^2} \frac{\partial^2 \Phi'}{\partial x_3'^2} = -\rho'(\mathbf{x}'), \qquad \rho'(\mathbf{x}') = \dfrac{v_b^2 \bar{f} q}{\varepsilon_0} \displaystyle\int_{\mathbb{R}^2_{v'}} f'(\mathbf{x}', \mathbf{v}')\, d\mathbf{v}' \\ \\ \bar{f} f'(t = 0, \mathbf{x}', \mathbf{v}') = f_0(\lambda x_1', \lambda x_2', L x_3', v_b v_1, v_b v_2). \end{cases} \tag{5}$$

It is natural to choose, as unit measure of the electric field

$$\bar{E} = \frac{mv_b^2}{qL};$$

moreover, since the third component of the electric field will play no role, its unity measure induces that

$$\bar{\Phi} = \bar{E}\lambda = \frac{m\lambda v_b^2}{qL}.$$

Finally, if we assume to have a small self consistent electric field, we are forced to work with a small density of particles. Therefore, we will assume that the dimensionless form of the density f is given by $f = \bar{f}\, f'$, with

$$\bar{f} = \frac{m\varepsilon_0}{q^2\lambda L}.$$

As mentioned in the introduction, we consider here low intensity beams so that the external electric field is much stronger than the self-consistent field. We translate this, introducing a small parameter ε, by saying that $\bar{\Xi}/\bar{E} = 1/\varepsilon$ and assuming that $\mathbf{\Xi}'$ writes

$$\mathbf{\Xi}' = \left[H_0\mathbf{G}_1 + \varepsilon H_1\left(\omega_1 \frac{Lx_3'}{l}\right)\mathbf{G}_2 \right],$$

where H_1 is $2\pi-$periodic and for a 2×2 isometric matrix $\mathbf{K}$

$$\mathbf{G}_1 = -\begin{pmatrix} x_1 \\ x_2 \\ 0 \end{pmatrix} \quad \text{and} \quad \mathbf{G}_2 = \begin{pmatrix} \mathbf{K} & 0 \\ 0 & 0 \end{pmatrix}\begin{pmatrix} x_1 \\ x_2 \\ 0 \end{pmatrix}.$$

On the other hand, we also suppose that the ratio between the average transverse radius of the beam and the longitudinal length of the accelerator $\lambda/L = \varepsilon$, and, that the ratio between the period of the external electric field and the macroscopic quantity $l/L = \varepsilon$. Forgetting the terms in ε^2, we have then obtained the dimensionless Vlasov-Poisson system in the paraxial approximation:

$$\begin{cases} \dfrac{\partial f'}{\partial x_3'} + \dfrac{1}{\varepsilon}\displaystyle\sum_{i=1}^{2} v_i' \frac{\partial f'}{\partial x_i'} + \sum_{i=1}^{2}\left(E_i' + \frac{1}{\varepsilon}\mathbf{\Xi}'\right)\frac{\partial f'}{\partial v_i'} = 0, \\ E_i' = -\partial\Phi'/\partial x_i', \qquad i = 1,2, \\ \displaystyle\sum_{i=1}^{2} \frac{\partial^2\Phi'}{\partial x_i'^2} = -\rho'(\mathbf{x}'), \qquad \rho'(\mathbf{x}') = \int_{\mathbb{R}^2_{v'}} f'(\mathbf{x}', \mathbf{v}')\, d\mathbf{v}', \\ f'(t=0, \mathbf{x}', \mathbf{v}') = f_0', \end{cases} \tag{6}$$

with

$$\frac{1}{\varepsilon}\mathbf{\Xi}' = -\frac{1}{\varepsilon}H_0\mathbf{G}_1 + H_1\left(\omega_1\frac{x_3'}{\varepsilon}\right)\mathbf{G}_2.$$

Denoting the variable x_3' with t (in order to have in (6) only two-dimensional vectors) and eliminating all the primed variables, we finally obtain the scaled Vlasov-Poisson paraxial system (1).

3 Main properties of the solution

We recall that, from now on, all the vectors are intended to be two-dimensional.

In the sequel, we will use heavily the property of boundedness of the solution with respect to some norms. This is guaranteed by the following lemma:

Lemma 3.1 *Let f_ε be the solution of the Vlasov-Poisson system* (1)*, with non-negative (a.e.) initial data f_0 of class $(L^1 \cap L^p)(\Omega)$, $p \geq 2$ and such that the moment of order two is finite:*

$$\int_\Omega (|\mathbf{x}|^2 + |\mathbf{v}|^2) f_0 \, d\mathbf{x}\, d\mathbf{v} < +\infty.$$

Then f_ε is bounded in $L^\infty([0,T]; L^p(\Omega))$ uniformly with respect to t. Moreover

$$\|(|\mathbf{x}|^2 f_\varepsilon + |\mathbf{v}|^2 f_\varepsilon)\|_{L^\infty([0,T];L^1(\Omega))} \leq C\, e^{\alpha T}, \tag{7}$$

with

$$\alpha = \frac{\varepsilon \|H_1\|_\infty}{\min\{1\,,\, H_0\}}.$$

Finally

$$\|\rho_\varepsilon(\mathbf{x},t)\|_{L^\infty([0,T];L^{\frac{3}{2}}(\mathbb{R}^3_x))} \leq C e^{\alpha T/3}, \tag{8}$$

for some constant C.

Proof: We multiply the Vlasov equation (1a) by f_ε^{p-1} and integrate in $\mathbf{x}$ and $\mathbf{v}$. We obtain

$$\|f^\varepsilon\|_{L^\infty([0,T];L^p(\Omega))} \leq C,$$

for some constant C. This proves the first part of the lemma.

In order to prove the other statements, we multiply the Vlasov equation (1a) by $|\mathbf{v}|^2$, and integrate with respect to $\mathbf{x}$ and $\mathbf{v}$. We get

$$\frac{d}{dt}\int_\Omega f_\varepsilon |\mathbf{v}|^2 \, d\mathbf{x}\, d\mathbf{v} - 2\int_{\mathbb{R}^2_x} \mathbf{J}\cdot(\mathbf{E}_\varepsilon + \boldsymbol{\Xi}^\varepsilon)\, d\mathbf{x} = 0, \tag{9}$$

where

$$\mathbf{J}(\mathbf{x},t) = \int_{\mathbb{R}^2_v} \mathbf{v} f_\varepsilon \, d\mathbf{v}.$$

Now, integrating the Vlasov equation in $\mathbf{v}$ gives the continuity equation

$$\frac{\partial \rho_\varepsilon}{\partial t} + \frac{1}{\varepsilon}\nabla\cdot\mathbf{J} = 0. \tag{10}$$

Thanks to the continuity equation (10), we note that

$$\int_{\mathbb{R}^2_x} \mathbf{J}\cdot\mathbf{E}_\varepsilon \, d\mathbf{x} = -\int_{\mathbb{R}^2_x} \mathbf{J}\cdot\nabla\Phi_\varepsilon \, d\mathbf{x} = \int_{\mathbb{R}^2_x} \nabla\cdot\mathbf{J}\,\Phi_\varepsilon \, d\mathbf{x} = -\varepsilon\int_{\mathbb{R}^2_x} \frac{\partial\rho_\varepsilon}{\partial t}\,\Phi_\varepsilon \, d\mathbf{x}. \tag{11}$$

Using now the Poisson equation, we get

$$\frac{1}{2}\frac{d}{dt}\int_{\mathbb{R}^2_x} (\nabla\Phi_\varepsilon)^2 \, d\mathbf{x} = -\int_{\mathbb{R}^2_x} \frac{\partial}{\partial t}(\Delta\Phi_\varepsilon)\,\Phi_\varepsilon \, d\mathbf{x} = \int_{\mathbb{R}^2_x} \frac{\partial\rho_\varepsilon}{\partial t}\,\Phi_\varepsilon \, d\mathbf{x}. \tag{12}$$

Coupling (11) and (12) we deduce:

$$-2\int_{\mathbb{R}^2_x} \mathbf{J}\cdot\mathbf{E}_\varepsilon\, d\mathbf{x} = \varepsilon\frac{d}{dt}\int_{\mathbb{R}^2_x}(\nabla\Phi_\varepsilon)^2\, d\mathbf{x}. \tag{13}$$

On the other hand, the external electric field $\mathbf{\Xi}^\varepsilon$ can be also derived from the potential

$$P(\mathbf{x}) = \frac{1}{2\varepsilon}H_0|\mathbf{x}|^2 - \frac{1}{2}H_1\left(\omega_1\frac{t}{\varepsilon}\right)\mathbf{K}\mathbf{x}\cdot\mathbf{x}.$$

A variant of the procedure used for the self-consistent field allows us to deduce

$$-2\int_{\mathbb{R}^2_x}\mathbf{J}\cdot\mathbf{\Xi}^\varepsilon\, d\mathbf{x} = 2\int_{\mathbb{R}^2_x}\mathbf{J}\cdot\nabla P\, d\mathbf{x} = -2\int_{\mathbb{R}^2_x}\nabla\cdot\mathbf{J}\, P\, d\mathbf{x} = 2\varepsilon\int_{\mathbb{R}^2_x}\frac{\partial\rho_\varepsilon}{\partial t}\, P\, d\mathbf{x} =$$

$$H_0\int_{\mathbb{R}^2_x}|\mathbf{x}|^2\frac{\partial\rho_\varepsilon}{\partial t}\, d\mathbf{x} - \varepsilon\int_{\mathbb{R}^2_x}H_1\left(\omega_1\frac{t}{\varepsilon}\right)\mathbf{K}\mathbf{x}\cdot\mathbf{x}\frac{\partial\rho_\varepsilon}{\partial t}\, d\mathbf{x},$$

and therefore (9) becomes

$$\frac{d}{dt}\left[\int f_\varepsilon|\mathbf{v}|^2\, d\mathbf{v}\, d\mathbf{x} + \varepsilon\int(\nabla\Phi_\varepsilon)^2\, d\mathbf{x} + H_0\int_{\mathbb{R}^2_x}|\mathbf{x}|^2\rho_\varepsilon\, d\mathbf{x}\right] =$$

$$= \varepsilon H_1\left(\omega_1\frac{t}{\varepsilon}\right)\int_{\mathbb{R}^2_x}\mathbf{K}\mathbf{x}\cdot\mathbf{x}\frac{\partial\rho}{\partial t}\, d\mathbf{x}.$$

If we multiply the Vlasov Equation (1a) by $|\mathbf{x}|^2$ and then integrate with respect to $\mathbf{x}$ and $\mathbf{v}$, we deduce that

$$\int_{\mathbb{R}^2_x}\mathbf{K}\mathbf{x}\cdot\mathbf{x}\,\frac{\partial\rho_\varepsilon}{\partial t}\, d\mathbf{x} = -\int_\Omega \mathbf{K}\mathbf{x}\cdot\mathbf{x}\,\mathbf{v}\cdot\nabla_x f_\varepsilon\, d\mathbf{x}\, d\mathbf{v} = 2\int_\Omega(\mathbf{K}\mathbf{x}\cdot\mathbf{v})\, f_\varepsilon\, d\mathbf{x}\, d\mathbf{v}$$

and thanks to the elementary inequality $2\mathbf{K}\mathbf{x}\cdot\mathbf{v} \le (|\mathbf{K}\mathbf{x}|^2 + |\mathbf{v}|^2) \le (|\mathbf{x}|^2 + |\mathbf{v}|^2)$, we obtain that

$$\frac{d}{dt}\left[\int_\Omega f_\varepsilon|\mathbf{v}|^2\, d\mathbf{v}\, d\mathbf{x} + \varepsilon\int_{\mathbb{R}^2_x}(\nabla\Phi_\varepsilon)^2\, d\mathbf{x} + H_0\int_{\mathbb{R}^2_x}|\mathbf{x}|^2\rho_\varepsilon\, d\mathbf{x}\right] \le$$

$$\le \varepsilon\|H_1\|_\infty\left[\int_\Omega|\mathbf{x}|^2 f_\varepsilon\, d\mathbf{x}\, d\mathbf{v} + \int_\Omega|\mathbf{v}|^2 f_\varepsilon\, d\mathbf{x}\, d\mathbf{v}\right].$$

Finally

$$\|(|\mathbf{x}|^2 f_\varepsilon + |\mathbf{v}|^2 f_\varepsilon)\|_{L^\infty([0,T];L^1(\Omega))} \le C\, e^{\alpha T},$$

with

$$\alpha = \frac{\varepsilon\|H_1\|_\infty}{\min\{1\,,\, H_0\}},$$

which proves the second statement of the lemma.

The proof of the bound on ρ_ε is a straightforward consequence of the following classical estimate (see for instance [11] (lemma 4.4)):

$$\int_{\mathbb{R}^2_x}|\rho_\varepsilon(\mathbf{x},t)|^{3/2}\, d\mathbf{x} \le C_3\left(\int_\Omega(f_\varepsilon)^2\, d\mathbf{x}\, d\mathbf{v}\right)^{1/2}\left(\int_\Omega|v|^2 f_\varepsilon\, d\mathbf{x}\, d\mathbf{v}\right)^{1/2}.$$

Hence the proof of the lemma is complete. □

4 Homogenization of the paraxial approximation

Our goal consists in deducing the equations satisfied by the limit of f_ε as $\varepsilon \to 0$. The homogenization of partial differential equations with rapidly periodic coefficients, as in the present case, can be fruitfully studied applying the two-scale convergence, introduced by N'guetseng [14] and subsequently developed by Allaire [2] and Frénod, Raviart and Sonnendrücker [9] and which essentially stands in the following theorem.

Theorem 4.1 *Let $\mathcal{Q}$ be a regular subset of $\mathbb{R}^n$, X a Banach space and X' its dual space, with $\langle\ ,\ \rangle$ as duality bracket. Let $1 < p \leq +\infty$ and p' be such that $\frac{1}{p} + \frac{1}{p'} = 1$ and let $Y = [0, a_1] \times \cdots \times [0, a_n]$ defined for finite real numbers a_i.*
If a sequence $(u_\varepsilon) = (u_\varepsilon(q))$ is bounded in $L^{p'}(\mathcal{Q}; X')$ then there exists a function $u_0 = u_0(q, y) \in L^{p'}(\mathcal{Q} \times Y; X')$ such that, up to a subsequence,

$$\lim_{\varepsilon \to 0} \int_{\mathcal{Q}} \left\langle u_\varepsilon(q), \nu\left(q, \frac{q}{\varepsilon}\right) \right\rangle dq = \int_{\mathcal{Q}} \int_Y \left\langle u_0(q, y), \nu\,(q, y) \right\rangle dqdy,$$

for any function $\nu \in L^p(\mathcal{Q}\,;\, C_Y(\mathbb{R}^n; X))$, where $C_Y(\mathbb{R}^n; X)$ stands for the space of continuous $Y-$periodic functions on $\mathbb{R}^n$ with values in X. We say that $(u_\varepsilon(x))$ two-scale converges to $u_0(x, y)$.

More precisely, we will use a theorem of Frénod and Sonnendrücker [11], which gives a generic framework, in the context of two-scale convergence, for linearly perturbed conservation laws of the form

$$\begin{cases} \dfrac{\partial u_\varepsilon}{\partial t} + \mathbf{A}^\varepsilon \cdot \nabla_x u_\varepsilon + \dfrac{1}{\varepsilon} \mathbf{L} \cdot \nabla_x u_\varepsilon = 0, \\ \\ u_\varepsilon(t = 0) = u_0. \end{cases} \tag{14}$$

In this system, $u^\varepsilon \equiv u^\varepsilon(t, \mathbf{x})$, $t \in [0, T)$ for some $T < \infty$ and $\mathbf{x} \in \mathbb{R}^n = \mathcal{O}$. Moreover it is assumed that, for all $\varepsilon > 0$, $\nabla_x \cdot \mathbf{A}^\varepsilon = 0$, and that, for some $q > 1$, $\mathbf{A}^\varepsilon \equiv \mathbf{A}^\varepsilon(t, \mathbf{x})$ two-scale converges to $\mathcal{A} \equiv \mathcal{A}(t, \tau, \mathbf{x}) \in L^\infty([0, T] \times [0, \theta]\,;\, W^{1,q}(K))$ for all compact sets $K \in \mathbb{R}^n$. Finally, $\mathbf{L} = M\mathbf{x}$ where M is a real $n \times n$ matrix with constant entries, satisfying $\mathrm{tr} M = 0$ and such that $e^{\tau M}$ is $\theta-$periodic.

Under these conditions, the following theorem is proved in [11]:

Theorem 4.2 *Under the assumptions above, if moreover the sequence (u_ε) of solution of (14) satisfies*

$$\|u_\varepsilon\|_{L^\infty([0,T];L^p(\mathcal{O}))} \leq C, \tag{15}$$

for some $p > 1$ such that $1/p + 1/q' < 1$, where $1/q' = \max\{1/q - 1/n\,,\, 0\}$, then, extracting a subsequence, u_ε two-scale converges to a profile

$$U \in L^\infty([0, T] \times [0, \theta]; L^p(\mathcal{O})).$$

Moreover we have

$$U(t, \tau, \mathbf{x}) = U_0(t, e^{-\tau M}\mathbf{x}), \tag{16}$$

where $U_0 \equiv U_0(t, \mathbf{y})$ is solution to

$$\begin{cases} \dfrac{\partial U_0}{\partial t} + \displaystyle\int_0^\theta e^{-\sigma M} \mathcal{A}(t, \sigma, e^{\sigma M}\mathbf{y})\, d\sigma \cdot \nabla_y U_0 = 0, \\ \\ U_0(t = 0) = \dfrac{1}{\theta} u_0. \end{cases} \tag{17}$$

The problem of homogenizing system (1) enters the framework we just presented with $\mathbf{x}$ replaced with $(\mathbf{x}, \mathbf{v}) \in \Omega$, with

$$\mathbf{A}^\varepsilon = \begin{pmatrix} 0 \\ \mathbf{E}_\varepsilon(t, \mathbf{x}) + H_1\big(\omega_1 \frac{t}{\varepsilon}\big)\, \mathbf{K}\mathbf{x} \end{pmatrix}, \tag{18}$$

and with

$$\mathbf{L} = \begin{pmatrix} \mathbf{v} \\ -H_0 \mathbf{x} \end{pmatrix} \text{ or in other words } M = \begin{pmatrix} 0 & I \\ -H_0 I & 0 \end{pmatrix}.$$

It is an easy game to see that

$$e^{\tau M} = \begin{pmatrix} \mathcal{R}_1(\tau) & \mathcal{R}_2(\tau)/\omega_0 \\ -\omega_0 \mathcal{R}_2(\tau) & \mathcal{R}_1(\tau) \end{pmatrix}, \text{ with } \omega_0 = \sqrt{H_0}, \tag{19}$$

where

$$\mathcal{R}_1(s) = \begin{pmatrix} \cos(\omega_0 s) & 0 \\ 0 & \cos(\omega_0 s) \end{pmatrix},$$

and

$$\mathcal{R}_2(s) = \begin{pmatrix} \sin(\omega_0 s) & 0 \\ 0 & \sin(\omega_0 s) \end{pmatrix}.$$

We can now prove:

Theorem 4.3 *Let f_0 satisfy the hypotheses of Theorem* 3.1. *Then, if we consider a sequence of solutions $(f_\varepsilon, \mathbf{E}_\varepsilon)$ depending on ε, extracting a subsequence, we have that f_ε two-scale converges to $F \in L^\infty([0,T] \times [0, \frac{2\pi}{\omega_0}]; L^2(\Omega))$ and $\mathbf{E}_\varepsilon$ two-scale converges to $\mathcal{E} \in L^\infty([0,T] \times [0, \frac{2\pi}{\omega_0}]; W^{1,3/2}(\mathbb{R}^2_x))$. Moreover, there exists a function $G = G(t, \mathbf{y}, \mathbf{u}) \in L^\infty([0,T]; L^2(\Omega))$ such that*

$$F(t, \tau, \mathbf{x}, \mathbf{v}) = G\left(t, \mathcal{R}_1(-\tau)\mathbf{x} + \frac{1}{\omega_0}\mathcal{R}_2(-\tau)\mathbf{v}\,,\, -\omega_0 \mathcal{R}_2(-\tau)\mathbf{x} + \mathcal{R}_1(-\tau)\mathbf{v}\right).$$

The pair $(G, \mathcal{E})$ is finally the solution of

$$\begin{cases} \dfrac{\partial G}{\partial t} + \dfrac{1}{\omega_0}\displaystyle\int_0^{2\pi/\omega_0} \mathcal{R}_2(-\sigma)\mathcal{E}(t, \sigma, \mathcal{R}_1(\sigma)\mathbf{y} + \frac{1}{\omega_0}\mathcal{R}_2(\sigma)\mathbf{u})\, d\sigma \cdot \nabla_y G \\ \qquad\qquad + \displaystyle\int_0^{2\pi/\omega_0} \mathcal{R}_1(-\sigma)\mathcal{E}(t, \sigma, \mathcal{R}_1(\sigma)\mathbf{y} + \frac{1}{\omega_0}\mathcal{R}_2(\sigma)\mathbf{u})\, d\sigma \cdot \nabla_u G = 0, \\ G(t=0) = \dfrac{\omega_0}{2\pi} f_0, \end{cases} \tag{20}$$

if $\omega_1/\omega_0 \notin \mathbb{Q}$ or if $H_1 = 0$ and

$$\begin{cases} \dfrac{\partial G}{\partial t} + \dfrac{1}{\omega_0}\displaystyle\int_0^{2\pi/\omega_0} \mathcal{R}_2(-\sigma)\Big[\mathcal{E}(t, \sigma, \mathcal{R}_1(\sigma)\mathbf{y} + \frac{1}{\omega_0}\mathcal{R}_2(\sigma)\mathbf{u}) \\ \qquad\qquad + \dfrac{\omega_0}{2\pi} H_1(\omega_1\sigma)\mathbf{K}\big(\mathcal{R}_1(\sigma)\mathbf{y} + \frac{1}{\omega_0}\mathcal{R}_2(\sigma)\mathbf{u}\big)\Big]\, d\sigma \cdot \nabla_y G \\ \qquad + \displaystyle\int_0^{2\pi/\omega_0} \mathcal{R}_1(-\sigma)\Big[\mathcal{E}(t, \sigma, \mathcal{R}_1(\sigma)\mathbf{y} + \frac{1}{\omega_0}\mathcal{R}_2(\sigma)\mathbf{u}) \\ \qquad\qquad + \dfrac{\omega_0}{2\pi} H_1(\omega_1\sigma)\mathbf{K}\big(\mathcal{R}_1(\sigma)\mathbf{y} + \frac{1}{\omega_0}\mathcal{R}_2(\sigma)\mathbf{u}\big)\Big]\, d\sigma \cdot \nabla_u G = 0, \\ G(t=0) = \dfrac{\omega_0}{2\pi} f_0, \end{cases} \tag{21}$$

if $\omega_1/\omega_0 \in \mathbb{N}$, *where* $\mathcal{E} = \mathcal{E}(t,\tau,\mathbf{x})$ *is solution to*

$$\begin{cases} \mathcal{E} = -\nabla\Psi, \\ -\Delta\Psi = \displaystyle\int_{\mathbb{R}^2_v} G\big(t, \mathcal{R}_1(-\tau)\mathbf{x} + \frac{1}{\omega_0}\mathcal{R}_2(-\tau)\mathbf{v}\,,\, -\omega_0\mathcal{R}_2(-\tau)\mathbf{x} + \mathcal{R}_1(-\tau)\mathbf{v}\big)\, d\mathbf{v}. \end{cases} \tag{22}$$

Proof: The deduction of this theorem follows directly from theorem 4.2 using the expression (19) of $e^{\tau M}$ once the two-scale convergence in A^ε given by (18) and in the Poisson equation (1c) is achieved.

As a direct consequence of estimates (7) and (8) and of the regularization properties of the Laplace operator, we deduce that $\mathbf{E}_\varepsilon$ is bounded in $L^\infty([0,T];W^{1,3/2}(\mathbb{R}^2_x))$, then, extracting a subsequence, $\mathbf{E}_\varepsilon$ two-scale converges to $\mathcal{E} = -\nabla\Psi \in L^\infty([0,T]\times[0,\frac{2\pi}{\omega_0}];W^{1,3/2}(\mathbb{R}^2_x))$.
In order to pass to the two-scale limit in the Poisson equation, we multiply it by a test function $\nu(t,\frac{t}{\varepsilon},\mathbf{x})$ such that $\tau\mapsto\nu(t,\tau,\mathbf{x})$ is $2\pi/\omega_0-$periodic, to give

$$\int_0^T\!\!\int_{\mathbb{R}^2_x} \nabla\Phi_\varepsilon(t,\mathbf{x})\cdot\nabla\nu(t,\frac{t}{\varepsilon},\mathbf{x})\,d\mathbf{x}dt = \int_0^T\!\!\int_\Omega f_\varepsilon(t,\mathbf{x},\mathbf{v})\,\nu(t,\frac{t}{\varepsilon},\mathbf{x})\,d\mathbf{x}d\mathbf{v}dt,$$

in which we pass to the limit to obtain

$$\begin{aligned}\int_0^{\frac{2\pi}{\omega_0}}\!\!\int_0^T\!\!\int_{\mathbb{R}^2_x} \nabla\Psi(t,\mathbf{x})\cdot\nabla\nu(t,\tau,\mathbf{x})\,d\mathbf{x}dtd\tau &= \int_0^{\frac{2\pi}{\omega_0}}\!\!\int_0^T\!\!\int_\Omega F(t,\tau,\mathbf{x},\mathbf{v})\nu(t,\tau,\mathbf{x})\,d\mathbf{x}d\mathbf{v}dtd\tau \\ &= \int_0^{\frac{2\pi}{\omega_0}}\!\!\int_0^T\!\!\int_\Omega G\left(t,\mathcal{R}_1(-\tau)\mathbf{x}+\mathcal{R}_2(-\tau)\mathbf{v}/\omega_0\,,\,-\omega_0\mathcal{R}_2(-\tau)\mathbf{x}+\mathcal{R}_1(-\tau)\mathbf{v}\right)\nu(t,\tau,\mathbf{x})\,d\mathbf{x}d\mathbf{v}dtd\tau,\end{aligned}$$

which is the weak formulation of (22).

On the other hand, if $\omega_1/\omega_0\notin\mathbb{Q}$, for any regular function ν which is $2\pi/\omega_0-$periodic in τ, the product

$$\int_0^T\!\!\int_{\mathbb{R}^2_x} H_1(\omega_1\frac{t}{\varepsilon})\mathbf{K}\mathbf{x}\cdot\nu(t,\frac{t}{\varepsilon},\mathbf{x})\,d\mathbf{x}dt \to 0,$$

since $\tau\mapsto H_1(\omega_1\tau)$ is $2\pi/\omega_1-$periodic with mean value 0. This yields equation (20).
If $\omega_1/\omega_0\in\mathbb{N}$, then $\tau\mapsto H_1(\omega_1\tau)$ is $2\pi/\omega_0-$periodic and

$$\int_0^T\!\!\int_{\mathbb{R}^2_x} H_1(\omega_1\frac{t}{\varepsilon})\mathbf{K}\mathbf{x}\cdot\nu(t,\frac{t}{\varepsilon},\mathbf{x})\,d\mathbf{x}dt \to \int_0^{\frac{2\pi}{\omega_0}}\!\!\int_0^T\!\!\int_{\mathbb{R}^2_x} H_1(\omega_1\tau)\mathbf{K}\mathbf{x}\cdot\nu(t,\tau,\mathbf{x})\,d\mathbf{x}dtd\tau,$$

yielding (21) and then ending the proof. □

Remark 4.4 *We can bring back the case* $\omega_1/\omega_0\in\mathbb{Q}\setminus\mathbb{N}$ *to the case* $\omega_1/\omega_0\in\mathbb{N}$ *by finding two integers* k *and* l *such that* $\omega_0' = \omega_0/k$ *and* $\omega_1' = \omega_1/l$ *satisfies* $\omega_1'/\omega_0'\in\mathbb{N}$ *and replacing in* (21) $\displaystyle\int_0^{2\pi/\omega_0} d\sigma$ *by* $\displaystyle\int_0^{2\pi/\omega_0'} d\sigma$.

We now turn to homogenizing system (3). For simplicity, we assume here that $\omega_0 = H_0 = 1$. We also assume that f_0 satisfies

$$f_0\geq 0, f_0\in(L^1\cap L^p)(\mathbb{R}^2;rdrdv_r) \text{ for } p\geq 2 \text{ and } \int_{\mathbb{R}^2}(r^2+v_r^2)f_0\,rdrdv_r < +\infty. \tag{23}$$

The considered system enters the framework presented in the beginning of the section with $\mathbf{x}$ replaced by $(r, v_r) \in \mathbb{R}^2$ with

$$\mathbf{A}^\varepsilon = \begin{pmatrix} 0 \\ \mathbf{E}_{r\varepsilon}(t,r) + H_1\big(\omega_1 \frac{t}{\varepsilon}\big)\, r \end{pmatrix}, \qquad \mathbf{L} = \begin{pmatrix} v_r \\ -r \end{pmatrix}, \tag{24}$$

$$M = \begin{pmatrix} 0 & 1 \\ -1 & 0 \end{pmatrix}, \qquad e^{\tau M} = \begin{pmatrix} \cos(\tau) & \sin(\tau) \\ -\sin(\tau) & \cos(\tau) \end{pmatrix}, \tag{25}$$

and the solution f_ε satisfies the needed estimates to deduce the following Theorem.

Theorem 4.5 *Under the assumptions above, extracting from a sequence of solution $(f_\varepsilon, \mathbf{E}_{r\varepsilon})$ to (3) a subsequence, we deduce that f_ε two-scale converges to $F \in L^\infty([0,T]\times[0,2\pi]; L^2(\mathbb{R}^2; r dr dv_r))$ and $\mathbf{E}_{r\varepsilon}$ two-scale converges to $\mathcal{E} \in L^\infty([0,T]\times[0,2\pi]; W^{1,3/2}(\mathbb{R}; r dr))$.*
Moreover, there exists a function $G = G(t,q,u_r) \in L^\infty([0,T]; L^2(\mathbb{R}^2; q dq du_r))$ such that

$$F(t,\tau,r,v_r) = G(t, \cos(\tau)r - \sin(\tau)v_r, \sin(\tau)r + \cos(\tau)v_r), \tag{26}$$

and G is solution to

$$\begin{cases} \dfrac{\partial G}{\partial t} + \displaystyle\int_0^{2\pi} -\sin(\sigma)\, \mathcal{E}_r(t,\sigma,\cos(\sigma)q + \sin(\sigma)u_r)\, d\sigma\, \dfrac{\partial G}{\partial q} \\ \qquad\qquad + \displaystyle\int_0^{2\pi} \cos(\sigma)\, \mathcal{E}_r(t,\sigma,\cos(\sigma)q + \sin(\sigma)u_r)\, d\sigma\, \dfrac{\partial G}{\partial u_r} = 0, \\ G(t=0) = \dfrac{1}{2\pi} f_0, \end{cases} \tag{27}$$

if $\omega_1/\omega_0 \notin \mathbb{Q}$ or if $H_1 = 0$ and

$$\begin{cases} \dfrac{\partial G}{\partial t} + \displaystyle\int_0^{2\pi} -\sin(\sigma)\Big(\mathcal{E}_r(t,\sigma,\cos(\sigma)q + \sin(\sigma)u_r) \\ \qquad\qquad + \dfrac{1}{2\pi} H_1(\omega_1\sigma)\big(\cos(\sigma)q + \sin(\sigma)u_r\big)\Big)\, d\sigma\, \dfrac{\partial G}{\partial q} \\ \qquad + \displaystyle\int_0^{2\pi} \cos(\sigma)\Big(\mathcal{E}_r(t,\sigma,\cos(\sigma)q + \sin(\sigma)u_r) \\ \qquad\qquad + \dfrac{1}{2\pi} H_1(\omega_1\sigma)\big(\cos(\sigma)q + \sin(\sigma)u_r\big)\Big)\, d\sigma\, \dfrac{\partial G}{\partial u_r} = 0, \\ G(t=0) = \dfrac{1}{2\pi} f_0, \end{cases} \tag{28}$$

if $\omega_1/\omega_0 \in \mathbb{N}$ where $\mathcal{E}_r = \mathcal{E}_r(t,\tau,r,v_r)$ is given by

$$\frac{1}{r}\frac{\partial(r\mathcal{E}_r)}{\partial r} = \Upsilon(t,\tau,r) = \int_{\mathbb{R}} G\big(t, \cos(\tau)r - \sin(\tau)v_r, \sin(\tau)r + \cos(\tau)v_r\big)\, dv_r\,. \tag{29}$$

5 The two scale PIC solver

In this section, we develop a two-scale PIC-method, tailored to approximate f_ε very efficiently on long time scales, in the simplified case of axisymmetric beams. The strategy consists in computing the solution F to (26)-(27)-(29) or (26)-(28)-(29) and then to approach the solution f_ε of (3) by $F(t, t/\varepsilon, \mathbf{x}, \mathbf{v})$. The advantage of proceeding in such a way is that the solution of (26)-(27)-(29) or (26)-(28)-(29) does not contain $1/\varepsilon-$frequency oscillations. As a consequence, a much larger time step may be used in the numerical method. First, we present the implemented algorithm. Then, we compare the solution obtained with our method with the solution f_ε directly computed from (3). Finally, we compare the performances of both methods.

5.1 Description of the numerical method

The Particle In Cell (PIC) method for the Vlasov-Poisson (or Vlasov-Maxwell) equations consists in approximating the distribution function defined in phase space by a meshless particle method and the electric field on a grid of the physical space only. In addition, adequate interpolation and charge deposition methods are used to transfer the needed quantities between grid and particles.

For the two-scale method we want to develop, the Vlasov-Poisson equation are replaced by equations (26)-(27)-(29) or (26)-(28)-(29).

The key point of the algorithm is the computation of function G solution to (27)-(29) or (28)-(29) at time $t_{l+1} = t_l + \Delta t$ knowing it at time t_l. We give the details of the method only in the case of system (27)-(29), knowing that in the case of system (28)-(29) ad-hoc terms need to be managed.

As usual in a PIC-method, G is approximated by the following Dirac mass sum

$$G_N(q,u,t) = \sum_{k=1}^{N} w_k \delta(q - Q_k(t))\delta(u - U_k(t)), \tag{30}$$

where $(Q_k(t), U_k(t))$ is the position in phase space of macro-particle k which moves along a characteristic curve of the first order PDE (27). Hence the job is reduced to compute the macro-particle positions (Q_k^{l+1}, U_k^{l+1}) at time $t_{l+1} = t_l + \Delta t$ from their positions (Q_k^l, U_k^l) at time t_l, knowing they are solutions to

$$\frac{dQ_k}{dt} = -\int_0^{2\pi} \sin(\sigma)\, \mathcal{E}_r(t, \sigma, \cos(\sigma)Q_k + \sin(\sigma)U_k)\, d\sigma, \qquad Q_k(t_l) = Q_k^l, \tag{31}$$

$$\frac{dU_k}{dt} = \int_0^{2\pi} \cos(\sigma)\, \mathcal{E}_r(t, \sigma, \cos(\sigma)Q_k + \sin(\sigma)U_k)\, d\sigma, \qquad U_k(t_l) = U_k^l. \tag{32}$$

These characteristic equations are a lot more complex to deal with than those of the standard Vlasov-Poisson system which read $\frac{dX}{dt} = V$, $\frac{dV}{dt} = E(X,t)$. Indeed, in our case Q and U are coupled in each equation and an integral term needs to be approximated.

Because of the form of the right hand side in (31) and (32) all along the algorithm, we need to compute values of the two-scale electric field $\mathcal{E}_r$ generated by a given macro-particle distribution $(Q_k, U_k)_{k=1,..,N}$. The tedious step while computing $\mathcal{E}_r$ in grid point $(q_i)_{i=1,..,A}$ is the computation of the right hand side $\Upsilon(t, \sigma_m, q_i)$ of (29). Indeed, $\Upsilon(t, \sigma_m, q_i)$ involves the integral of the particle distribution on the oblique line which is the range of the vertical line $[q = q_i]$ by the rotation $e^{-\sigma_m M}$ defined by (25). Hence we have to apply this rotation to each line $[q = q_i]$ and to project the particles $(Q_k, U_k)_{k=1,..,N}$ on the resulting oblique lines. Summing then the projection result on the oblique line associated with q_i yields the value of $\Upsilon(t_l, \sigma_m, q_i)$. Another way to obtain this value consists in applying the rotation $e^{\sigma_m M}$ to the particles, then projecting this rotation result on lines $[q = q_i]$ and summing. Once $\Upsilon(t_l, \sigma_m, q_i)$ is known in each q_i, the computation of the $\mathcal{E}_r(t_l, \sigma_m, q_i)$ are straightforward using any classical Poisson numerical solver.

The first step of the computation of (Q_k^{l+1}, U_k^{l+1}) consists in replacing the integrals above by $p-$node quadrature formula. As we approximate the integral of a periodic function over one period, the trapezoidal rule is optimal and will yield very accurate results for as few quadrature points as are needed to resolve the oscillations of the function.

Then, the equations for (Q_k, U_k) become

$$\frac{dQ_k}{dt} = -\sum_{m=1}^{p} \gamma_m \sin(\sigma_m)\, \mathcal{E}_r(t, \sigma_m, \cos(\sigma_m)Q_k + \sin(\sigma_m)U_k), \quad Q_k(t_l) = Q_k^l, \tag{33}$$

$$\frac{dU_k}{dt} = \sum_{m=1}^{p} \gamma_m \cos(\sigma_m)\, \mathcal{E}_r(t, \sigma_m, \cos(\sigma_m)Q_k + \sin(\sigma_m)U_k), \quad U_k(t_l) = U_k^l. \tag{34}$$

Then, we solve (33)-(34) using the classical Runge-Kutta method:

$$\begin{array}{c|cccc} 0 & & & & \\ 1/2 & 1/2 & & & \\ 1/2 & 0 & 1/2 & & \\ 1 & 0 & 0 & 1 & \\ \hline & 1/6 & 1/3 & 1/3 & 1/6 \end{array} \tag{35}$$

which gives the following scheme when applied to the computation of the approximation y^{l+1} of the value of y solution to $dy/dt = K(t, y)$ at time $t_l + \Delta t$ knowing its approximation y^l at time t_l:

$$\begin{aligned} &t_{l,1} = t_l, \quad y^{l,1} = y^l \\ &t_{l,2} = t_l + \frac{\Delta t}{2}, \quad y^{l,2} = y^l + \frac{1}{2} I^1, \text{ with } I^1 = \Delta t\, K(t_{l,1}, y^{l,1}), \\ &t_{l,3} = t_l + \frac{\Delta t}{2}, \quad y^{l,3} = y^l + \frac{1}{2} I^2, \text{ with } I^2 = \Delta t\, K(t_{l,2}, y^{l,2}), \\ &t_{l,4} = t_l + \Delta t, \quad y^{l,4} = y^l + I^3, \text{ with } I^3 = \Delta t\, K(t_{l,3}, y^{l,3}), \end{aligned} \tag{36}$$

$$y^{l+1} = y^l + \frac{1}{6} I^1 + \frac{1}{3} I^2 + \frac{1}{3} I^3 + \frac{1}{6} I^4 \text{ with } I^4 = \Delta t\, K(t_{l,4}, y^{l,4}).$$

Applying this scheme to our problem consists in replacing in the formula above y by (Q_k, U_k) and computing K using the result of a Poisson solver. In other words, we have to compute $Q_k^{l,2}$ as follows:

$$\begin{aligned} &Q_k^{l,2} = Q_k^l + \frac{1}{2} I^1, \text{ with} \\ &I^1 = \Delta t \Big(- \sum_{m=1}^{p} \gamma_m \sin(\sigma_m)\, \mathcal{E}_r(t_l, \sigma_m, \cos(\sigma_m)Q_k^l + \sin(\sigma_m)U_k^l) \Big). \end{aligned} \tag{37}$$

and something similar for $U_k^{l,2}$.

In order to achieve this, we compute the value of $\mathcal{E}_r$ in $(t_l, \sigma_m, \cos(\sigma_m)Q_k^l + \sin(\sigma_m)U_k^l)$ by interpolating the value of $\mathcal{E}_r(t_l, \sigma_m, q_i)$ known on the grid $(q_i)_{i=1..,A}$ as soon as it has been computed solving the Poisson equation (29) associated with the particle distribution (Q_k^l, U_k^l) by the procedure described above.

The following step of the Runge-Kutta method consists in computing $Q_k^{l,3}$ defined by

$$\begin{aligned} &Q_k^{l,3} = Q_k^l + \frac{1}{2} I^2, \text{ with} \\ &I^2 = \Delta t \Big(- \sum_{m=1}^{p} \gamma_m \sin(\sigma_m)\, \mathcal{E}_r^2(t_l + \frac{\Delta t}{2}, \sigma_m, \cos(\sigma_m)Q_k^{l,2} + \sin(\sigma_m)U_k^{l,2}) \Big), \end{aligned} \tag{38}$$

where the value of $\mathcal{E}_r^2(t_l + \frac{\Delta t}{2}, \sigma_m, \cos(\sigma_m)Q_k^{l,2} + \sin(\sigma_m)U_k^{l,2})$ is obtained by interpolation of $\mathcal{E}_r^2(t_l + \frac{\Delta t}{2}, \sigma_m, q_i)$ which is computed as previously from the $(Q_k^{l,2}, U_k^{l,2})_{k=1,..,N}$ particle distribution.

Then we compute

$$Q_k^{l,4} = Q_k^l + I^3, \text{ with}$$
$$I^3 = \Delta t\Big(- \sum_{m=1}^{p} \gamma_m \sin(\sigma_m)\, \mathcal{E}_r^3(t_l + \frac{\Delta t}{2}, \sigma_m, \cos(\sigma_m) Q_k^{l,3} + \sin(\sigma_m) U_k^{l,3})\Big), \tag{39}$$

where $\mathcal{E}_r^3(t + \frac{\Delta t}{2})$ is computed from particle positions $(Q_k^{l,3}, U_k^{l,3})_{k=1,..,N}$.

Finally, Q_k^{l+1} is obtained by the following formula:

$$Q_k^{l+1} = Q_k^l + \frac{1}{6} I^1 + \frac{1}{3} I^2 + \frac{1}{3} I^3 + \frac{1}{6} I^4, \text{ with}$$
$$I^4 = \Delta t\Big(- \sum_{m=1}^{p} \gamma_m \sin(\sigma_m)\, \mathcal{E}_r^4(t_l + \Delta t, \sigma_m, \cos(\sigma_m) Q_k^{l,4} + \sin(\sigma_m) U_k^{l,4})\Big). \tag{40}$$

where I^1, I^2 and I^3 are defined above and where $\mathcal{E}_r^4(t_l + \Delta t)$ is computed from particle positions $(Q_k^{l,4}, U_k^{l,4})_{k=1,..,N}$.

5.2 Validation of the two-scale solver

The linear case. First in order to check our implementation we consider the case when the self-consistent electric field vanishes. Then by choosing adequately the function H_1 we can compute an analytical solution of the two-scale model that we can compare with our code and with the solution given by the usual PIC solver.

Let us first consider the non resonant case by choosing $H_1(t) = \cos(4\sqrt{2}t)$. In this case, as the self-consistent electric field vanishes, G is stationary and the beam will only move through the rotation transforming G to F. We check on figure 1 that this is indeed the case. Let us now consider the resonant case by choosing $H_1(t) = \cos^2(nt)$ with $n \geq 2$. Then a straightforward computation yields the equation satisfied by G

$$\frac{\partial G}{\partial t} - \frac{1}{4} u \frac{\partial G}{\partial q} + \frac{1}{4} q \frac{\partial G}{\partial u}.$$

The characteristics of this equation can be computed explicitly:

$$Q(t) = Q_0 \cos\frac{t}{4} - U_0 \sin\frac{t}{4}, \quad U(t) = Q_0 \sin\frac{t}{4} + U_0 \cos\frac{t}{4},$$

which yields an explicit solution of G and also an explicit solution of F using formula (26). Comparing this exact solution with the solution computed by our solver we can check its accuracy. Let us first mention, that our quadrature formula yields the exact result up to machine accuracy for any number of quadrature points greater or equal to seven for $n = 2$ in the definition of H_1. Of course when the chosen n is larger the function oscillates more and more quadrature points are needed. For $n = 7$, for example, the exact result, up to machine accuracy, is obtained with 17 quadrature points. We can thus conclude that as long as the oscillations are resolved our quadrature rule is very accurate. We also check that our RK solver is of order 4 in Δt as expected. In figure 2, we check the global behavior for a whole beam in comparison to the usual PIC solver and the results are very satisfying. The phase shift appearing in the two-scale limit is indeed also observed in the usual PIC code. Note that because the usual PIC code needs to resolve the fast time scale, the difference in time step between of the two solvers is of the order of ϵ, so that the efficiency of the two-scale PIC solver compared to the usual PIC solver is better for small values of ϵ.

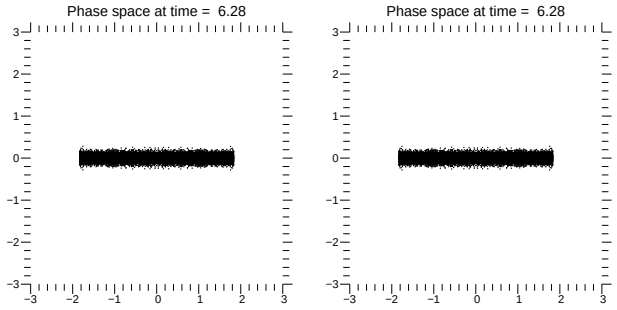

Figure 1: Beam simulation without self-consistent electric field in the non resonant case ($H_1(t) = \cos(4\sqrt{2}t)$) with a usual PIC method (left) and a two-scale PIC method (right) for $\varepsilon = 0.01$ at time 6.28.

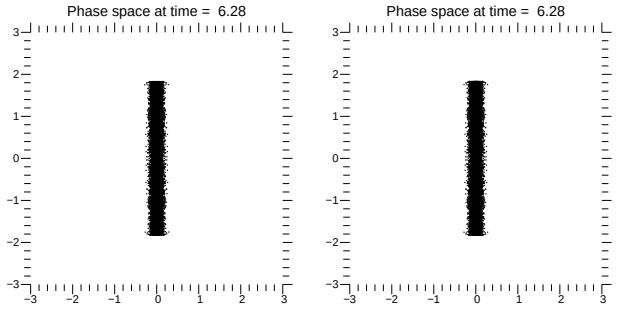

Figure 2: Beam simulation without self-consistent electric field in the resonant case ($H_1(t) = \cos^2(2t)$) with a usual PIC method (left) and a two-scale PIC method (right) for $\varepsilon = 0.01$ at time 6.28.

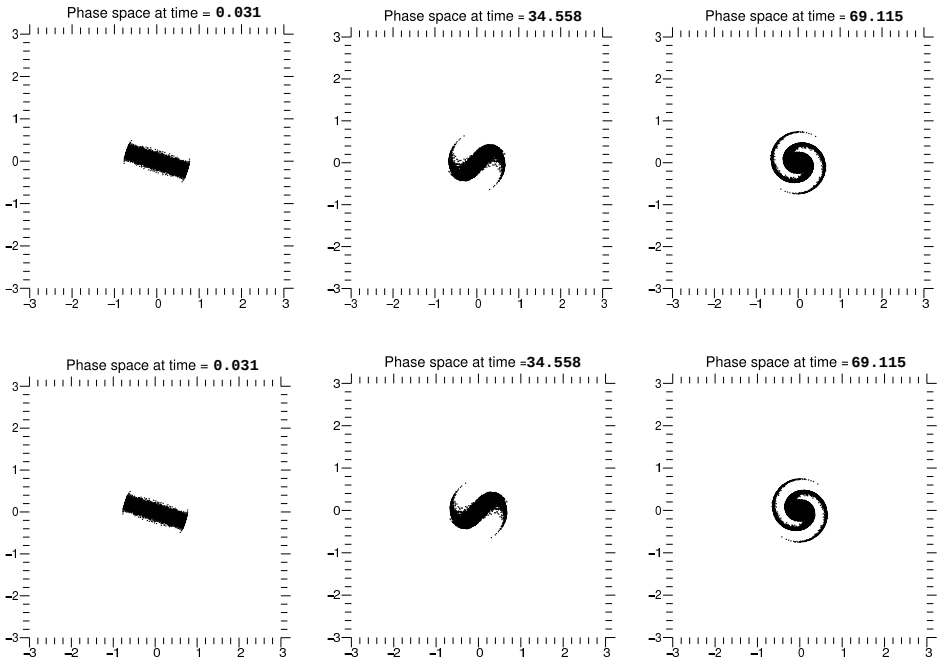

Figure 3: Beam simulation with a usual PIC method and a two-scale PIC method for $\varepsilon = 0.01$. Left: beam at time 0.031, center: beam at time 34.558, right : beam at time 69.115. Top : Simulation provided with the usual PIC method, bottom: Simulation provided with the two-scale PIC method.

The non linear case. In this case, as no analytical solution is available, we shall compare our solver with a traditional PIC solver resolving the small time scale.

Let us first consider a case of a fairly small ε on which we test our two-scale PIC method, where the two scale solution should be fairly close to the solution given by the traditional PIC solver. We take $\varepsilon = 0.01$, and choose as an initial distribution

$$f_0(r, v_r) = \frac{n_0}{\sqrt{2\pi} v_{th}} exp\Big(- \frac{v_r^2}{2v_{th}^2} \Big) \chi_{[-0.75,0.75]}(r), \tag{41}$$

with thermal velocity $v_{th} = 0.0727518214392$ and where $\chi_{[-0.75,0.75]}(r) = 1$ if $r \in [-0.75, 0.75]$ and 0 otherwise and in considering function H_1 as being identically zero. This corresponds to a semi-Gaussian beam often used in accelerator physics. We consider in all our simulations beams which are willingly unmatched in order to assess to what extent our two-scale PIC solver can follow the complex structures that are developing.

We use a 15-node composed trapezoidal quadrature formula. The results are given in figure 3 where the horizontal axis is the r axis and the vertical axis the v_r axis. The top line shows the time evolution of the beam simulated with a usual standard PIC method and the bottom line shows the same simulation with the two-scale PIC method just built. We can see that the two simulations coincide with a high degree of accuracy. The time step in the two-scale PIC method is ε times larger as in the usual PIC method. The simulations were both made with an Intel Core 2 Duo processor (2.33 GHz) under Mac OS X 10.4.10 (8R2218) system. The needed CPU time for the simulation with the usual standard PIC method is 4320.382 seconds and is 549.197 seconds with the two-scale PIC method.

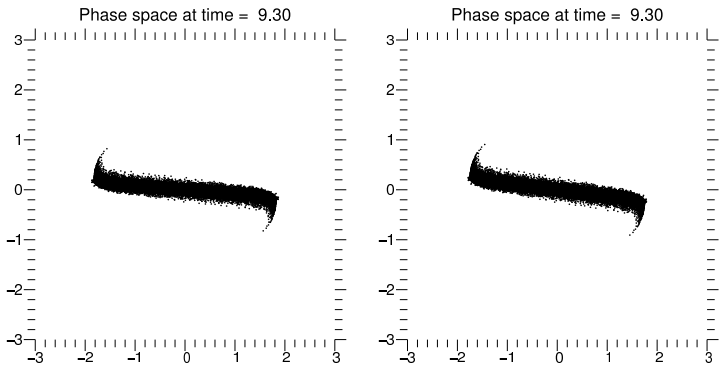

Figure 4: Beam simulation with an external force with no mean effect at time 9.30. Left: with the usual PIC method. Right: with the two-scale PIC method.

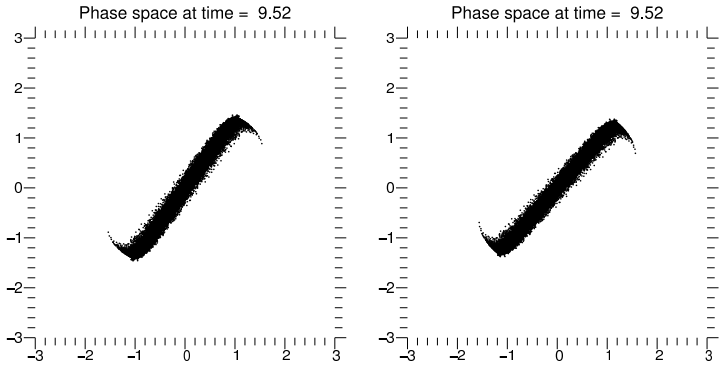

Figure 5: Beam simulation with an external force with no mean effect at time 9.52. Left: with the usual PIC method. Right: with the two-scale PIC method.

The three next tests are done with $\varepsilon = 0.1$ and with initial distribution

$$f_0(r, v_r) = \frac{n_0}{\sqrt{2\pi} v_{th}} exp\Big(- \frac{v_r^2}{2v_{th}^2} \Big) \chi_{[-1.83271471003, 1.83271471003]}(r), \tag{42}$$

with thermal velocity $v_{th} = 0.0727518214392$. In the case when

$$H_1(\omega_1 \tau) = \cos(\tau), \tag{43}$$

the mean effect of it is zero in the sense that terms containing H_1 appearing in (28) are both zero.
Numerical results concerning this case are given in figures 4 and 5. On the left of both figures is shown the simulation result with a usual PIC method. On the right is shown the simulation result with the two-scale PIC method. We can notice that if the beam configuration are very similar at time 9.30 (figure 4) the two-scale PIC method is a bit in advance at time 9.52 (figure 5). This illustrates a finite ε effect making that the two-scale PIC method is sometimes late and sometimes in advance with respect to the usual PIC method.

The case when

$$H_1(\omega_1 \tau) = \cos^2(\tau), \tag{44}$$

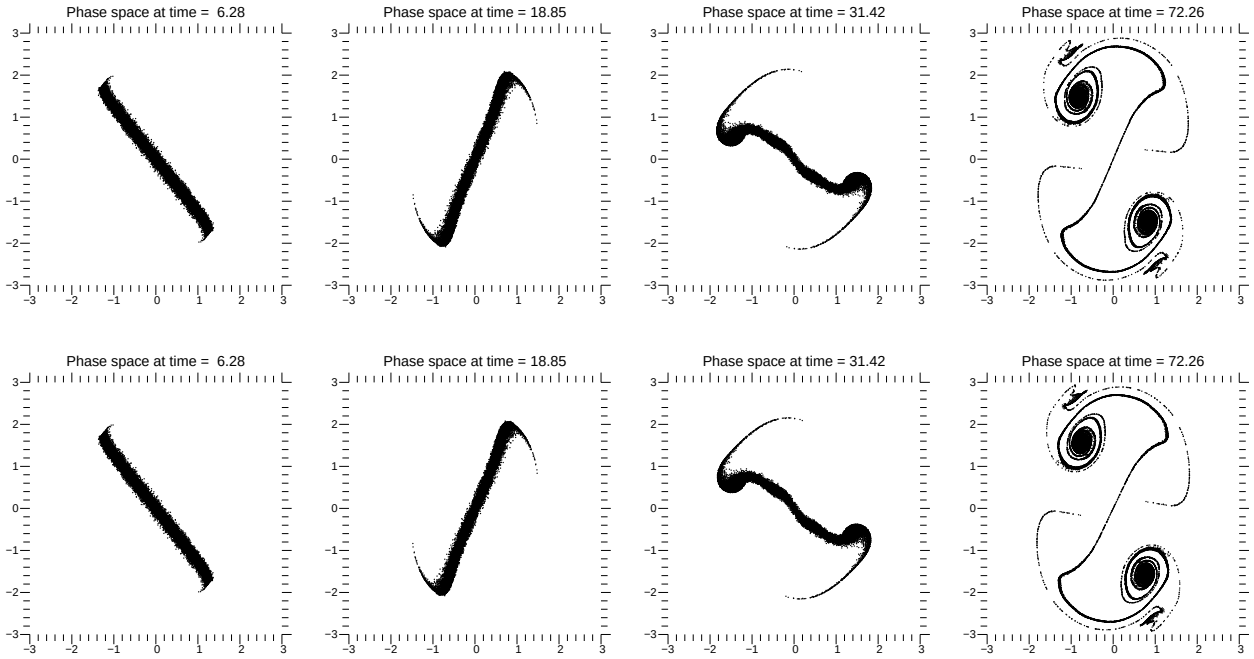

Figure 6: Left: beam at time 6.26, center left: beam at time 18.85, center right : beam at time 31.42, right : beam at time 72.26. Top : Simulation provided with the usual PIC method, bottom: Simulation provided with the two-scale PIC method.

generates a real effect on the long term. In other words, the terms containing H_1 in (28) are

$$\frac{1}{2\pi}\int_0^{2\pi} \sin(\sigma)\cos^2(\sigma)\big(\cos(\sigma)q + \sin(\sigma)u_r\big)\,d\sigma = -\frac{1}{8}u_r, \tag{45}$$

$$\frac{1}{2\pi}\int_0^{2\pi} \cos(\sigma)\cos^2(\sigma)\big(\cos(\sigma)q + \sin(\sigma)u_r\big)\,d\sigma = \frac{3}{8}q. \tag{46}$$

The simulation results are given in figure 6. The top line shows the time evolution of the beam simulated with a usual standard PIC method and the bottom line shows the same simulation with the two-scale PIC method just built. The simulations coincide with a good degree of accuracy also in this case.

Finally we consider the case when

$$H_1(\omega_1\tau) = \cos(2\tau), \tag{47}$$

which has a defocusing effect on the beam as

$$\frac{1}{2\pi}\int_0^{2\pi} \sin(\sigma)\cos(2\sigma)\big(\cos(\sigma)q + \sin(\sigma)u_r\big)\,d\sigma = \frac{u_r}{4}, \tag{48}$$

$$\frac{1}{2\pi}\int_0^{2\pi} \cos(\sigma)\cos(2\sigma)\big(\cos(\sigma)q + \sin(\sigma)u_r\big)\,d\sigma = \frac{q}{4}. \tag{49}$$

The result shown in figure 7 shows that also in this case the two-scale PIC method gives results that are qualitatively and quantitatively very close to those of the usual PIC method.

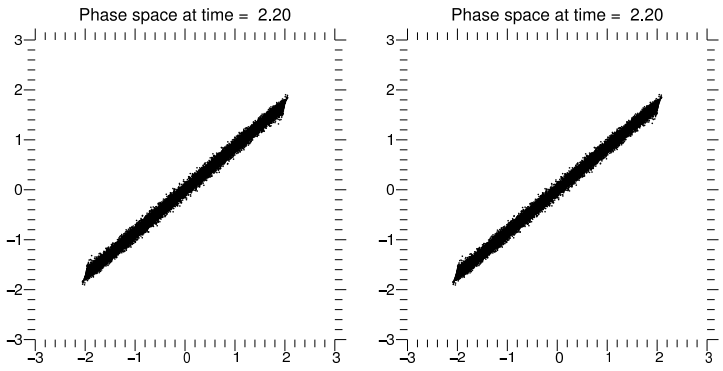

Figure 7: Beam simulation with an external de-focusing force at time 2.20. Left: with the usual PIC method. Right: with the two-scale PIC method.

6 Conclusions and perspectives

We have developed and validated a new PIC solver that can deal very efficiently with a problem involving two time scales. The two-scale solver is based on homogenized equations that have been obtained analytically in our application. For small values of ϵ the new solver can follow as accurately as the original solver the complex structure of the particle distribution that is generated in a mismatched particle beam in an accelerator at a small fraction of the cost of the usual PIC solver. These numerical results obtained in 1D are very promising and the extension to more dimensions as well as the used of semi-Lagrangian or other type of solvers for the Vlasov-like equation instead of a PIC solver deserve to be investigated for accelerator physics as well as for other applications, e.g. strongly magnetized plasmas where the fast motion along the magnetic field lines provides a fast time scale. On the other hand, a similar two time scale method can probably also be applied in cases where the homogenized equation can only be computed numerically.

Acknowledgments: The authors acknowledge financial support from the project HYKE, "Hyperbolic and Kinetic Equations: Asymptotics, Numerics, Analysis" financed by the European Union under Contract Number HPRN-CT-2002-00282. The second author thanks the Université Louis Pasteur, where this paper has been partially written, for hospitality.

References

[1] P. Ailliot, E. Frénod, V. Monbet. Long term object drift forecast in the ocean with tide and wind. *Multiscale Modeling and Simulation* **5**-2 (2006), 514–531

[2] G. Allaire. Homogenization and two-scale convergence, *SIAM J. Math. Anal.*, **23**-6 (1992), 1482-1518

[3] R. Davidson, H. Qin. Physics of intense charged particle beams in high energy accelerators *Imperial College Press and World Scientific*, Singapore, 2001

[4] P. Degond, P. A. Raviart. On the paraxial approximation of the stationary Vlasov-Maxwell system, *Math. Models Methods Appl. Sci.* **3**-4 (1993), 513-562

[5] E. Frénod. Homogénéisation d'équations cinétiques avec potentiels oscillants, *PhD Thesis* (1994)

[6] E. Frénod. Application of the averaging method to the gyrokinetic plasma, *Asymp. Anal.* **46**-1 (2006), 1-28

[7] E. Frénod, A. Mouton, E. Sonnendrücker Two-scale numerical simulation of the weakly compressible 1D isentropic Euler equations, *Numer. Math.* (In press)

[8] E. Frénod, K. Hamdache. Homogenisation of Kinetic Equations with Oscillating Potentials *Proc. Royal Soc. Edinburgh* **126 A** (1996) 1247–1275

[9] E. Frénod, P. A. Raviart, E. Sonnendrücker. Asymptotic Expansion of the Vlasov Equation in a Large External Magnetic Field, *J. Math. Pures et Appl.*, **80**-8 (2001), 815-843

[10] E. Frénod, E. Sonnendrücker. Homogenization of the Vlasov Equation and of the Vlasov-Poisson System with a strong External Magnetic Field *Asymp. Anal.* **18**-3,4 (1998) 193–214

[11] E. Frénod, E. Sonnendrücker. The finite Larmor radius approximation, *SIAM J. Math. Anal.*, **32**-6 (2001), 1227-1247

[12] F. Filbet, E. Sonnendrücker. Modeling and Numerical Simulation of Space Charge Dominated Beams in the Paraxial Approximation, *Math. Models Methods Appl. Sci.* **16**-5 (2006), 763-791

[13] R. T. Glassey. The Cauchy problem in kinetic theory, *Society for Industrial and Applied Mathematics (SIAM)*, Philadelphia, 1996

[14] G. N'Guetseng. A general convergence result for a functional related to the theory of homogenization, *SIAM J. Math. Anal.*, **20**-3 (1989), 608-623